Structure of the 70-kDa Soluble Lytic Transglycosylase Complexed with Bulgecin A. Implications for the Enzymic Mechanism

ARTICLE *in* BIOCHEMISTRY · NOVEMBER 1995

Impact Factor: 3.02 · DOI: 10.1021/bi00039a032 · Source: PubMed

4 AUTHORS, INCLUDING:

Henriette J Rozeboom
University of Groningen
68 PUBLICATIONS **3,397** CITATIONS
SEE PROFILE

Kor H. Kalk
University of Groningen
151 PUBLICATIONS **9,891** CITATIONS
SEE PROFILE

Bauke W. Dijkstra
University of Groningen
339 PUBLICATIONS **17,076** CITATIONS
SEE PROFILE

Structure of the 70-kDa Soluble Lytic Transglycosylase Complexed with Bulgecin A. Implications for the Enzymatic Mechanism†

Andy-Mark W. H. Thunnissen,‡ Henriëtte J. Rozeboom, Kor H. Kalk, and Bauke W. Dijkstra*

Laboratory of Biophysical Chemistry and BIOSON Research Institute, Department of Chemistry, University of Groningen, Nijenborgh 4, 9747 AG Groningen, The Netherlands

Received June 5, 1995; Revised Manuscript Received August 1, 1995⊗

ABSTRACT: Bulgecins are O-sulfonated glycopeptides that are able to enhance the antibacterial activity of β-lactam antibiotics. The 70-kDa soluble lytic transglycosylase (SLT70) from *Escherichia coli* forms a specific target of these compounds. Using X-ray crystallography, the three-dimensional structure of a complex of SLT70 with bulgecin A has been determined to 2.8-Å resolution and refined to an *R* factor of 19.5%. The model contains all 618 amino acids of SLT70 and a single molecule of bound bulgecin, located in the active site of the enzyme. The glycopeptide inhibitor is bound in an extended conformation occupying sites analogous to the B, C, and D subsites of lysozyme. Upon binding of bulgecin, the three-stranded antiparallel β-sheet in the C domain shows a pronounced shift toward the inhibitor. In subsite D, the proposed catalytic residue Glu478 forms a hydrogen bond to the hydroxymethyl oxygen of the proline part of bulgecin and interacts electrostatically with the proline NH_2^+ group. These interactions, in addition to the interactions observed for the 2-acetamido group of the *N*-acetylglucosamine residue bound in subsite C, may explain the strong inhibition of SLT70 activity by bulgecin, suggesting that bulgecin acts as an analogue of an oxocarbonium ion intermediate in the reaction catalyzed by SLT70. The structure of the SLT70−bulgecin A complex may be of assistance in the rational design of novel antibiotics.

The lytic transglycosylases from *Escherichia coli* are a group of bacterial exomuramidases involved in the metabolism of the cell wall peptidoglycan. These enzymes catalyze the cleavage of the β-1,4-glycosidic bond between *N*-acetylmuramic acid (MurNAc)[1] and *N*-acetylglucosamine (GlcNAc) residues. Whereas lysozymes accomplish the cleavage by hydrolyzing the glycosidic bonds, the lytic transglycosylases carry out an intramolecular glycosyl transferase reaction resulting in the formation of 1,6-anhydromuropeptides (Höltje et al., 1975). Different functions for the lytic transglycosylases have been suggested (Höltje & Tuomanen, 1991), including a role as space maker for the insertion of new peptidoglycan material during growth and remodeling of the cell wall, a role as cell wall zipper during cell division, and a function in the recycling of old peptidoglycan material. Since the activity of these enzymes is potentially suicidal for the organism (Kitano et al., 1986), it must be under strict control, and it must be precisely coordinated with the action of peptidoglycan-synthesizing enzymes for orderly growth and division of the cell without disrupting the integrity of the cell wall. The mechanisms by which the bacterium accomplishes these highly sophisticated tasks are still far from understood.

Three different lytic transglycosylases have been isolated from *E. coli*, two are soluble proteins located in the periplasmic space with molecular masses of 70 and 35 kDa (Höltje et al., 1975; Engel et al., 1992), the other is a membrane-bound protein of 38 kDa (Romeis et al., 1993; Ursinus & Höltje, 1994). The 70-kDa soluble lytic transglycosylase (SLT70) has been studied in most detail, both biochemically (Beachey et al., 1981; Keck et al., 1985; Kusser & Schwarz, 1980) and genetically (Betzner & Keck, 1989; Engel et al., 1991). Recently, the three-dimensional structure has been obtained by X-ray crystallography (Thunnissen et al., 1994). The crystal structure of SLT70 is composed of three domains, two of which form a novel "superhelical" ring of α-helices, while the third C-terminal domain has a lysozyme-like fold. The active site of SLT70 is located in the C-terminal domain. While Glu478 has been proposed to have a similar role as the "catalytic" glutamic acid in lysozymes, SLT70 lacks the catalytic aspartate residue that is commonly found in the active site of lysozymes. From a comparison with the three distinct types of lysozyme (chicken, phage, goose-type) with known three-dimensional structure, it could be shown that the C-domain of SLT70 defines a novel bacterial-type lysozyme (Dijkstra & Thunnissen, 1995; Thunnissen et al., 1995) that is characterized by the occurrence of a limited number of differences in the arrangement of secondary structure elements and by the absence of an aspartate in the catalytic site. The closest relationship was found with the structure of a member of the goose-type lysozymes. Interestingly, as was shown recently (Weaver, 1995), the goose-type lysozymes also lack a catalytic aspartate residue.

† This work was supported by the Netherlands Organization for Scientific Research and the Netherlands Foundation for Chemical Research.

* To whom correspondence should be addressed. Fax: +31-50-3634800.

‡ Present address: Melvin Calvin Laboratory, Structural Biology Division, Chemistry Department, University of California at Berkeley, Berkeley CA 94720.

⊗ Abstract published in *Advance ACS Abstracts,* September 15, 1995.

[1] Abbreviations: SLT70, 70-kDa soluble lytic transglycosylase (*Escherichia coli*); HEWL, hen egg white lysozyme; T4L, lysozyme from bacteriophage T4; GlcNAc, *N*-acetylglucosamine; MurNAc, *N*-acetylmuramic acid; F_o, observed structure factor amplitudes; F_c, calculated structure factor amplitudes; rms, root-mean-square; σ, standard deviation.

0006-2960/95/0434-12729$09.00/0

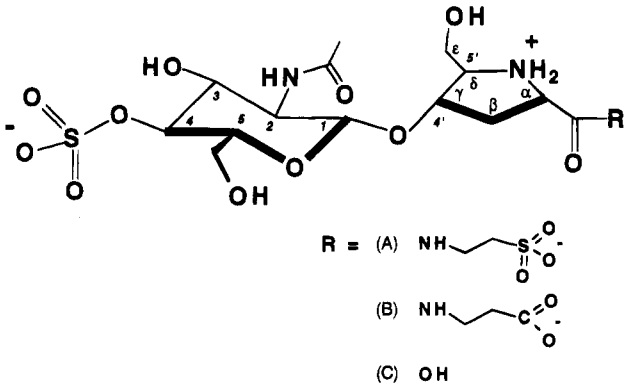

FIGURE 1: Structure of bulgecins. Bulgecins consist of a 4-*O*-sulfonyl-*N*-acetylglucosamine residue that is linked with a semi-β-1,4-glycosidic linkage to a 4-hydroxy-5-(hydroxymethyl)-L-proline. Bulgecins are produced by *P. acidophila* and *P. mesoacidophila* in three different forms, A–C, which differ in the moiety that is linked to the carboxylic group of the proline. Bulgecin A constitutes the major component. It contains a taurine residue, which is linked to the proline via an amide bond. In bulgecin B the proline is linked to a β-alanine, whereas in bulgecin C the proline has a free carboxylic group.

Little is known about the catalytic mechanism of SLT70. Also the functional importance of SLT70 is still unclear. The enzyme is no target for β-lactam antibiotics. *E. coli* mutants that lack the SLT70 gene do not show a specific phenotype and grow normally under standard conditions (Templin et al., 1992). This result, however, may be explained by the redundancy that exists in the set of peptidoglycan-degrading enzymes in *E. coli* (Höltje & Tuomanen, 1991), and the function of SLT70 may be taken over by the other lytic transglycosylases. Interestingly, the SLT70-deficient mutants are much more sensitive toward β-lactam antibiotics than normal cells and form bulges prior to rapid bacteriolysis when exposed to β-lactams. Similar morphological alterations occur in wild-type *E. coli* cells when the β-lactams are combined with compounds known as bulgecins. These are a group of O-sulfonated glycopeptides produced by *Pseudomonas acidophila* and *Pseudomonas mesoacidophila* (Shinagawa et al., 1985) (Figure 1). Although by themselves bulgecins are devoid of any antibacterial activity, in combination with β-lactam antibiotics they induce bulge formation in the cell wall of Gram-negative bacteria and potentiate the lytic activity of the β-lactam antibiotics. It has been shown that one of the bulgecins (bulgecin A) specifically inhibits SLT70 (Templin et al., 1992), thus explaining the similar susceptibility toward antibiotics of SLT70-deficient *E. coli* strains and of *E. coli* bacteria grown in the presence of bulgecin.

To understand the structural basis for the mode of inhibition by bulgecin, and to increase our understanding of the catalytic function of the lytic transglycosylases, we have determined the structure of the SLT70–bulgecin A complex by X-ray crystallography at 2.8-Å resolution. The results clearly show that bulgecin A is bound in the active site of SLT70 interacting with the catalytic Glu478. The structure of the complex suggests that bulgecin mimics the oxocarbonium ion intermediate.

MATERIALS AND METHODS

Preparation and Data Collection of the SLT70–Bulgecin Crystals. Crystallization of native SLT70 crystals has been described previously (Rozeboom et al., 1990). Crystals of SLT70 belong to spacegroup $P2_12_12_1$ with a = 80.8 Å, b = 88.4 Å, and c = 132.6 Å and contain one molecule per asymmetric unit. Crystals of the SLT70–bulgecin complex were obtained by soaking native crystals for 48 h at room temperature in a solution of 40% saturated $(NH_4)_2SO_4$ in 0.1 mM NaOAc, pH 5.0, containing 7 mM bulgecin A. Initially, data from 25 to 3.1 Å were collected on an Enraf-Nonius FAST area detector mounted on a Elliot GX-21 rotating anode X-ray generator operating at 40 kV and 75 mA. Data processing was carried out with the MADNES software system (Messerschmidt & Pflugrath, 1987), complemented with Kabsch profile fitting (Kabsch, 1988). Merging of the data into a unique set of structure factor amplitudes was performed with programs of the BIOMOL (Groningen, The Netherlands) software package. The structure factor amplitudes of the SLT70–bulgecin A complex were scaled to the native SLT70 data using the program KBRANI (BIOMOL), and an $F_{o,complex} - F_{o,native}$ difference map at 3.5-Å resolution was calculated with observed structure factor amplitudes and phases calculated from the native structure. This map clearly indicated the presence of the bulgecin in the putative active site of SLT70. A new data set of the complex was collected to 2.8-Å resolution on the image plate system at beamline X31 of the EMBL Outstation at the DESY synchrotron, Hamburg. The image plate data were processed with the MOSFLM software (Leslie, A. G. W, MRC, Cambridge, UK) and merged with programs from the CCP4 package (Collaborative Computational Project Number 4, 1994). The synchrotron data set was used in the refinement of the SLT70–bulgecin complex. A summary of the data collection and processing statistics is given in Table 1.

Table 1: Statistics of Data Collection and Processing

data set	FAST	image plate
X-ray source,[a] wavelength (Å)	ROTA, 1.542	SYN, 1.003
no. of crystals	2	4
cell parameters (Å)		
a	79.70	80.31
b	88.24	88.47
c	132.4	133.1
resolution range (Å)	25–3.10	22–2.80
no. of unique data	15997	23903
data redundancy	1.9	4.8
completeness (%)	90	99
R_{merge}[b]	8.7	8.0
R_{iso}[c]	20.4	23.4

[a] ROTA, rotating anode; SYN, synchrotron. [b] $R_{merge} = \sum_{hkl}\sum_{refl,j}|I_{(hkl,j)} - \bar{I}_{(hkl)}|/\sum_{hkl}\sum_{refl,j}\bar{I}_{(hkl)}$. [c] $R_{iso} = \sum||F_{o,bulgecin}| - |F_{o,native}||/\sum|F_{o,native}|$.

Structure Refinement. The structure of the SLT70–bulgecin complex was refined starting from the native model of SLT70 (Thunnissen et al., 1994). The initial R factor was 29% with all data from 8 to 2.8 Å. First, a three-dimensional rigid-body refinement of this model in the 8–3.5-Å resolution range was carried out using the program X-PLOR (Brünger, 1992a). Next, the protein model, still without the inhibitor, was subjected to a few rounds of positional refinement against data from 8.0 to 2.8 Å with $|F_o| > 2\sigma$ using the "conventional" energy minimization routine in X-PLOR. The significance of the refinement was continuously monitored by cross-validation with the free R factor (Brünger, 1992b), which was calculated from 10% of the data omitted from the refinement. Small adjustments were made to the protein model, and addition of the bulgecin

Table 2: Refinement Statistics for SLT70−Bulgecin A Complex

resolution range (Å)	8.0−2.80
R factors (no. of reflections)[a]	
R_{all}	0.195 (22746)
R_{work}	0.185 (20119)
R_{free}	0.268 (2207)
no. of protein atoms	4965
no. of water molecules	0
no. of bulgecin atoms	35
RMS deviations from ideality[b]	
bond distances (Å)	0.015
angles (deg)	2.9
dihedrals (deg)	21
improper dihedrals (deg)	1.4
average *B* factors[c] (Å^2)	
main chain	21.4 (2.3)
side chain	26.9 (5.4)
bulgecin	18.7 (3.2)

[a] *R* factor $= \sum||F_o| - |F_c||/\sum|F_o|$. R_{all} is calculated for all reflections in the resolution range. R_{work} and R_{free} are defined for reflections with $|F| > 2\sigma$. R_{free} has been calculated from reflections that were not included in the actual refinement. [b] With respect to Engh and Huber (1991) parameter set. [c] The values in parentheses are the average deviations in *B* factors between bonded atoms.

inhibitor was based on $F_o - F_c$ and $2F_o - F_c$ Fourier maps. The glycopeptide inhibitor was built from the X-ray coordinates of a desulfated form of bulgecin A (Shinagawa et al., 1984) using the program BIOGRAF version 3.1 (Molecular Simulations Inc., Waltham, MA) and adjusted manually to fit the difference electron density using the program O (Jones et al., 1991). A topology file was constructed for the glycopeptide inhibitor together with a file containing the force constants and parameters necessary to restrain the geometry of bulgecin A during the refinement. Then, the model of the SLT70−bulgecin complex was optimized by further rounds of positional and *B*-factor refinement. Table 2 contains a summary of the refinement statistics. No water molecules were added to the model.

Structure Analysis. Assessment of the stereochemical quality of the protein model was carried out using the PROCHECK program (Laskowski et al., 1993). Further analysis of the SLT70−bulgecin structure was done with programs of the BIOMOL and CCP4 software packages. Figures 4, 5a, 6, and 8 were produced with MOLSCRIPT (Kraulis, 1991). Coordinates of the SLT70−bulgecin A complex have been deposited with the Brookhaven Protein Data Bank (entry 1SLY).

RESULTS

Accuracy of the SLT70−Bulgecin Model. The refined model of the SLT70−bulgecin complex has a crystallographic *R* factor of 19.5% for all data between 8 and 2.8 Å with good geometry (Table 2). The *R* factors for the working set and the free set of reflections [R_{work} and R_{free}; Brünger (1992b)] are 18.5% and 26.8%, respectively. Electron density for the protein backbone is well defined except for residues 371−377, which form part of a flexible loop at the surface of the protein. The average *B* factors for main-chain and side-chain atoms are 21.4 and 26.9 Å^2, respectively. Analysis of the (φ, ψ) dihedral angles (Morris et al., 1992) shows that 499 (90.2%) of the non-glycine and non-proline residues are in the most favored regions, while the other 54 residues (9.8%) are in the additional allowed regions. No amino acid residues are found in a disallowed region. The estimated rms coordinate error, derived from a σ_A plot (Read, 1986), is ~0.4 Å. From the $F_o - F_c$ difference electron map (Figure 2A) it can be seen that, except for the taurine part, the inhibitor has well-defined electron density. The S4, C7, O, C5, and OH atoms occupy peaks in the electron density map of 19, 11, 11, 9, and 8 times the standard deviation, respectively. The average *B* factor for the bulgecin atoms, excluding those of the taurine moiety, is 12.9 Å^2, while the average *B* factor for the taurine atoms is 41.8 Å^2.

Interactions between Bulgecin and the Active Site of SLT70. The crystal structure of native SLT70 has been previously described (Thunnissen et al., 1994). Bulgecin A is bound to SLT70 at a single site per protein molecule (Figure 2B), located in the region of the active site cleft that is analogous to subsites B, C, and D of the lysozymes (Thunnissen et al., 1995). The inhibitor adopts an extended conformation with the 4-*O*-sulfonate group of the GlcNAc residue located at subsite B, the GlcNAc bound in subsite C, and the proline residue bound in subsite D. The taurine part of bulgecin A that is linked to the proline points outward from subsite D toward the solvent. Specific interactions between bulgecin A and SLT70 occur in both subsites C and D (Figure 3; Table 3). The 4-*O*-sulfonate group of GlcNAc in subsite B makes no direct hydrogen bonds with any protein atoms and is largely accessible to solvent. It may be that binding of this group occurs through water molecules, but the resolution of the SLT70−bulgecin complex does not allow the identification of such interactions. The sulfonate group is positioned at ~4 Å from the N-terminus of helix Cα6 [residues 556−559 of SLT70; Thunnissen et al. (1994)], coinciding with the helical axis. This suggests that it may have an electrostatic interaction with the α-helix dipole moment (Hol, 1985). In addition, the position of the sulfonate group might be stabilized by an intramolecular hydrogen bond interaction with the O6 of the GlcNAc residue; the distance between this atom and one of the sulfonate oxygens is 2.8 Å.

In subsite C, the 2-acetamido group of the GlcNAc residue is bound between two backbone segments of SLT70 with hydrogen bonds from the N2 atom to the main-chain C=O of Tyr552, and from the O7 atom to the main-chain NH of Met498. In addition, a strong van der Waals contact is made by the C8 methyl group and the side chain of Tyr552. Adjacent to the 2-acetamido group, the 3-hydroxy O3 of GlcNAc makes hydrogen bonds with the side chains of Tyr533 and Thr501, respectively. The 5-hydroxymethyl group of GlcNAc is not involved in any hydrogen bond with protein atoms.

In subsite D, the hydroxymethyl oxygen of the proline residue of bulgecin makes a direct hydrogen bond with the Oε2 atom of the catalytic Glu478. Another hydrogen bond occurs between the carbonyl oxygen of the proline and the side chain of Ser487. Furthermore, an electrostatic interaction might occur between the amine of the proline and the side chain of Glu478. The amine is located ~4 Å away from the Oε1 atom of Glu478. Since it has a pK_a higher than 9 [Hall (1957) and *Handbook of Biochemistry* (1968)], at the pH of this experiment (pH 5) we would expect this group to bear two protons and a net positive charge. In the SLT70−bulgecin complex, the side chain of Glu478 is most probably ionized, thereby stabilizing the NH_2^+ group of the bulgecin.

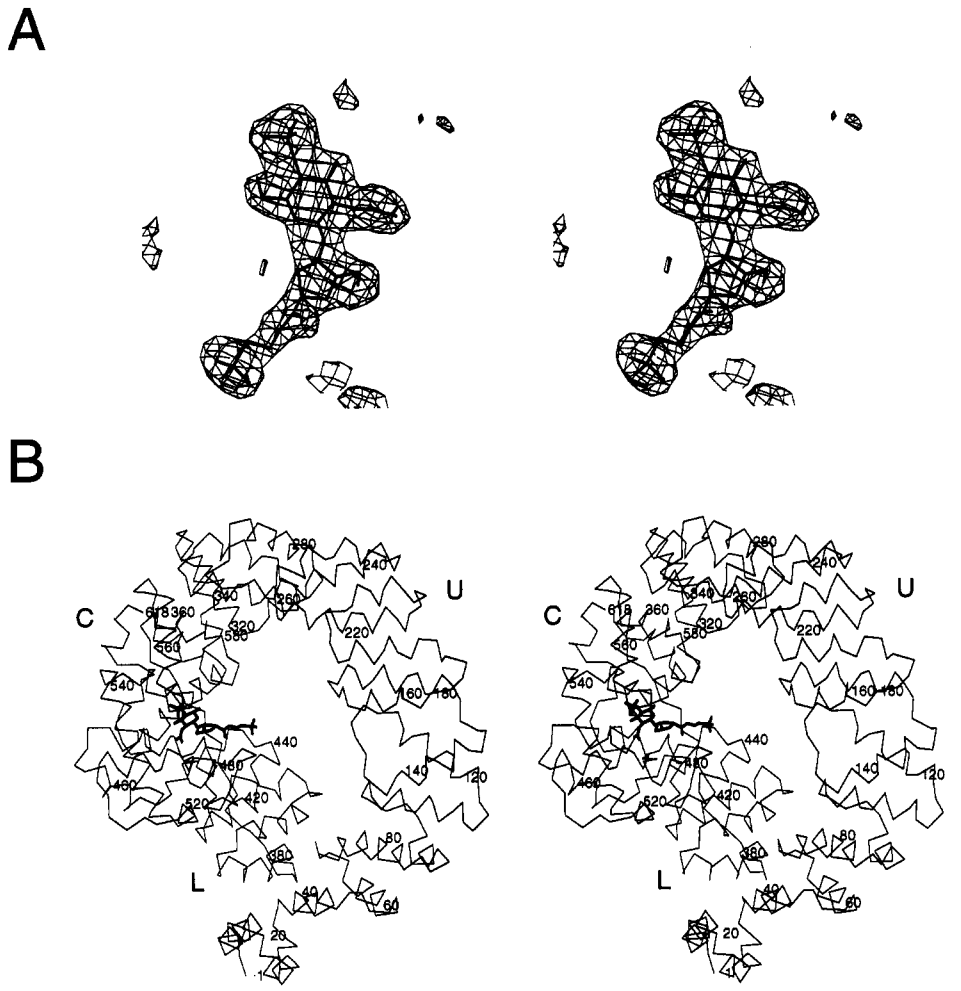

FIGURE 2: (A) Stereoview of final $F_o - F_c$ difference electron density for bulgecin in the active site of SLT70 at 2.8-Å resolution. Only the protein atoms of the SLT70−bulgecin complex were included in the F_c calculations. The map is contoured at 3σ of the electron density. (B) Stereofigure showing the Cα backbone (thin lines) of SLT70 with bound bulgecin A (thick lines). Every twentieth amino acid residue has been numbered. The binding site of bulgecin is located in the C domain of SLT70 (residues 449−618). The U domain (residues 1−360) and L domain (residues 381−448) make a superhelical ring that forms the basis of the SLT70 doughnut. No binding of bulgecin was observed to the latter two domains.

The taurine part of the inhibitor forms only a few contacts with protein atoms, including a hydrogen bond between the amide N3 and the side chain of Glu583. Most of the sulfonate group of the taurine is accessible to solvent.

Conformational Changes Associated with the Binding of Bulgecin. Upon binding of bulgecin, the antiparallel β-sheet of SLT70 moves toward the inhibitor (Figure 4). Compared to the uncomplexed SLT70, the β-sheet (residues 483−499) shows an overall rms difference in position of 1.0 Å for main-chain atoms and 1.1 Å for side-chain atoms (for all 618 residues of SLT70 these numbers are 0.4 and 0.6 Å, respectively). Movement of the backbone is most pronounced for the first two β-strands at subsite D, with a maximum shift of up to 2 Å occurring at Pro489 and Val490 in the β1−β2 turn. The movement of the β-sheet optimizes the contacts with bulgecin. In particular, the side chain of Ser487 moves to a position where it is able to form a hydrogen bond with the carbonyl O of the proline part of bulgecin. Due to the concerted movement of all three strands, the hydrogen-bonding network of the β-sheet is not distorted.

Apart from the movement of the β-sheet, there are no dramatic changes in the conformation of residues around the bulgecin binding site. The nine side chains, which have at least one atom within 4.0 Å from bulgecin, excluding those in the β-sheet, show a rms difference in atomic positions of only ~0.5 Å. These displacements are not substantially greater than the estimated coordinate error.

DISCUSSION

Mode of Inhibition of Bulgecin A. The observed binding mode of bulgecin A is hard to associate with a noncompetitive inhibition of SLT70 activity, as was suggested by a previous study (Templin et al., 1992). Our results clearly demonstrate that bulgecin is an active site inhibitor. The affinity of bulgecin for the active site of SLT70 can be explained by the structural similarity of this compound to the disaccharide subunit of peptidoglycan. The hydrogen bonds and hydrophobic interactions of the acetamido group in subsite C are the same as observed in lysozymes complexed with inhibitors (Weaver et al., 1985). At subsite D, the interactions of Glu478 with the hydroxymethyl group and the NH_2^+ group of the proline part of bulgecin may also contribute significantly to the binding, explaining the strong inhibition of SLT70 by bulgecin: already 50% of the SLT70 activity is lost in the presence of 0.42 μM bulgecin (Templin et al., 1992). In fact, the hydrogen-bonding distance between

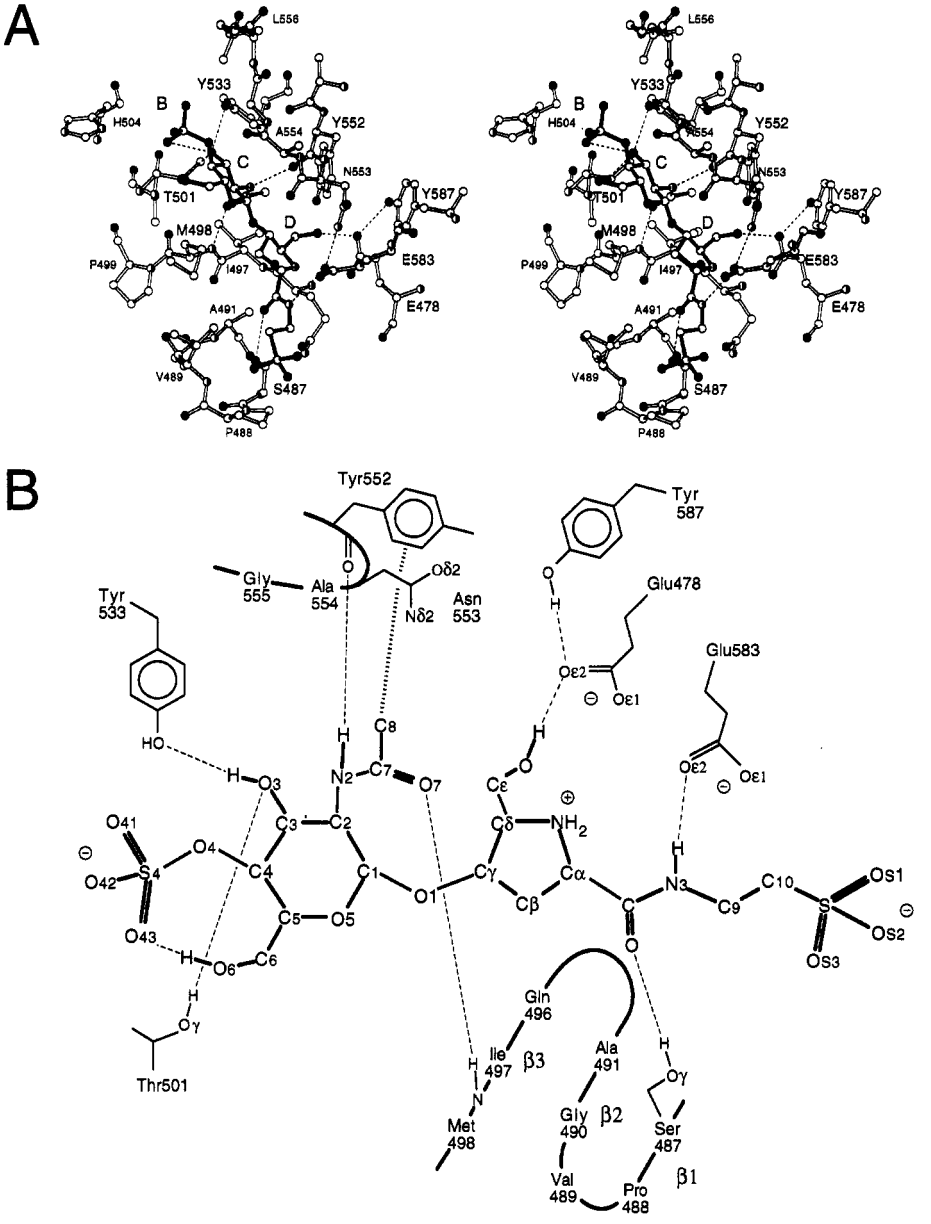

FIGURE 3: Protein–inhibitor interactions in the SLT70–bulgecin complex. (A) Stereodiagram showing the refined structure of bulgecin in the active site cleft of SLT70. Inferred hydrogen bonds are shown as thin dotted lines. Oxygen atoms are shown filled, nitrogen atoms half-filled, and carbon atoms as open circles. (B) Schematic illustration of the inferred interactions between bulgecin and SLT70, including the van der Waals contact between the 2-acetamidomethyl group of GlcNAc in subsite C and the side chain of Tyr552.

Table 3: Summary of Bulgecin–Protein Interactions

		inferred hydrogen bonds[a]			
	subsite	bulgecin atom	protein atom	distance (Å)	residues in van der Waals contact[b]
S-GlcNAc	C	N2	Tyr552 O	2.9	Ile497 Met498 Thr501
		O7	Met498 N	2.8	Tyr533 Tyr552 Asn553
		O3	Thr501 Oγ1	3.2	Ala554 Gly555 Leu556
			Tyr533 OH	2.8	
proline	D	OH	Glu478 Oϵ2	2.5	Glu478 Val489 Ala491
		O	Ser487 Oγ	2.9	Gln496 Tyr552 Asn553
taurine		N3	Glu583 Oϵ2	3.3	Pro488 Val489 Glu583

[a] The maximum length of an allowed hydrogen bond was 3.3 Å. [b] Van der Waals contacts are defined for distances less than 4 Å, excluding possible hydrogen bond interactions.

the catalytic Glu478 and the hydroxymethyl oxygen of bulgecin's proline at subsite D is the shortest of all putative hydrogen-bonding interactions of bulgecin, suggesting a strong interaction. The presence of the hydroxymethyl group at the proline is essential for the inhibition of SLT70 by bulgecin, since bulgecin lacking this group does not show any synergistic activity with β-lactam antibiotics (Wakamiya et al., 1987).

Bulgecin Mimicking of the Oxocarbonium Ion Reaction Intermediate. In the proposed mechanism for hen egg white lysozyme (HEWL) (Blake et al., 1967; Phillips, 1967) the catalytic glutamic acid (Glu35) acts as a general acid that

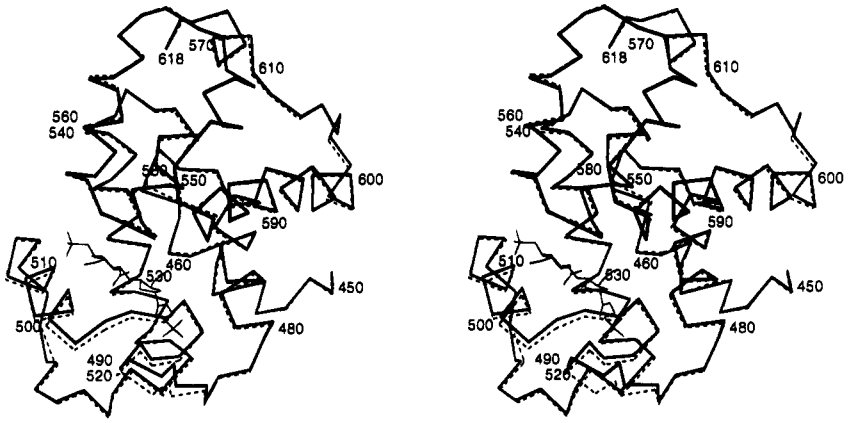

FIGURE 4: Stereoview showing a three-dimensional superposition of the Cα backbones of the C domain in the SLT70−bulgecin complex (thick lines) and uncomplexed, native SLT70 (dashed lines). Bulgecin is also shown. Note the movement of the β-sheet toward the inhibitor.

donates a proton to the glycosidic oxygen of the scissile bond, resulting in bond cleavage and formation of an oxocarbonium ion intermediate. Formation of the oxocarbonium ion intermediate is favored and stabilized by the steric distortion of the MurNAc residue bound in subsite D from a low-energy chair conformation toward a higher energy half-chair or sofa conformation and by the electrostatic interaction with the carboxylate group of the catalytic aspartate (Asp52). Subsequently, the leaving group at subsite E diffuses away from the active site and is replaced by a water molecule. This water molecule, presumably activated by Glu35, then attacks the C1 carbon atom of the oxocarbonium ion, thus completing the reaction with retention of configuration at C1. Over the past years the proposed mechanism of lysozyme has been the subject of several controversies. Especially the stabilizing role of the catalytic aspartate and the proposed steps involving the ground-state distortion of the D sugar have been debated. For the lysozyme from bacteriophage T4 (T4L), at least two different mechanisms have been proposed with the catalytic aspartate acting as a nucleophile to generate a covalent glycosyl−enzyme intermediate (Hardy & Poteete, 1991; Koshland, 1953) or as a base activating a water molecule for nucleophilic attack in a single displacement reaction (Kuroki et al., 1993). The conformation of the sugar in subsite D has been controversial due to lack of experimental evidence. However, in the last three years, three independent high-resolution X-ray diffraction studies of different lysozyme−oligosaccharide complexes have been reported which clearly show a distorted sugar residue in subsite D (Hadfield et al., 1994; Kuroki et al., 1993; Strynadka & James, 1991).

A possible reaction mechanism for SLT70, compared to that for HEWL, is shown in Figure 5. Since SLT70 lacks the catalytic aspartic acid and, moreover, produces nonreducable 1,6-anhydromuropeptides, at least in some aspects the reaction mechanism of SLT70 has to be different from that of HEWL. The first step of the reaction, formation of an oxocarbonium ion intermediate, may be similar, with Glu478 in SLT70 having a role equivalent to Glu35 in HEWL. The next reaction steps, however, are likely to be different. Instead of a water molecule, the C6-hydroxyl group of the MurNAc performs an intramolecular nucleophilic attack on the C1 carbon of the oxocarbonium ion in SLT70. Such an attack requires that the glycosidic ring of the oxocarbonium ion adopts a boat conformation with the C5-hydroxymethyl group in an axial position (Figure 5). Only then the C6-hydroxyl group will be able to optimally approach the C1 carbon for a nucleophilic attack. The catalytic Glu478 may assist in the activation of the C6-hydroxyl group by abstracting its proton. As mentioned earlier (Thunnissen et al., 1994), the intramolecular nucleophilic attack by the C6-hydroxyl group would probably require a shorter lifetime of the oxocarbonium intermediate, and thus less stabilization, as it is no longer dependent on the diffusion-controlled replacement of the leaving group with a water molecule, explaining why there is no need for a catalytic aspartate in SLT70. Alternatively, the oxocarbonium ion could be stabilized by a favorable interaction with the carbonyl oxygen atom of the *N*-acetyl group of the substrate (see below).

The structure of the SLT70−bulgecin complex provides support for several of the proposed steps of the reaction mechanism. Close examination of the bulgecin structure reveals that the proline part of the inhibitor mimics the oxocarbonium intermediate. The conformation of the proline ring with Cα, Cδ, Cγ, and the ring nitrogen almost coplanar and the semiaxial position of the hydroxymethyl group *trans* to the Cγ−O1 substituent is very similar to the sofa conformation of the oxocarbonium sugar. Furthermore, the charge distribution in the proline with a positive charge on the nitrogen is similar to that in the oxocarbonium ion, where the positive charge is delocalized between C1 and O5. Therefore, the interactions of the proline part of bulgecin in subsite D may be relevant for the interactions that play a role in the reaction mechanism of SLT70. To explore this possibility further, we modeled a GlcNAc−MurNAc disaccharide with the sugar ring of MurNAc in a sofa conformation on the basis of the observed binding of bulgecin to SLT70. Coordinates of the disaccharide were obtained from the X-ray structure of the complex of a T4L mutant with a cell wall muropeptide from *E. coli* (Kuroki et al., 1993). The result of the model building is shown in Figure 6. If the GlcNAc of the disaccharide is fixed to the position of GlcNAc of bulgecin in subsite C, the MurNAc sugar in subsite D fits remarkably well on the proline of bulgecin, without any need to rotate the β-1,4-glycosidic bond. In the superposed structures, the C2, C3, C4, and C5 atoms in the MurNAc ring of the disaccharide are very close to the Cα, Cβ, Cγ, and Cδ atoms of the proline ring of bulgecin, while the nitrogen of the proline ring is located in between the C1 and O5 atoms of the glucose ring. Moreover, the 5-hydroxymethyl group of MurNAc occupies a position equiva-

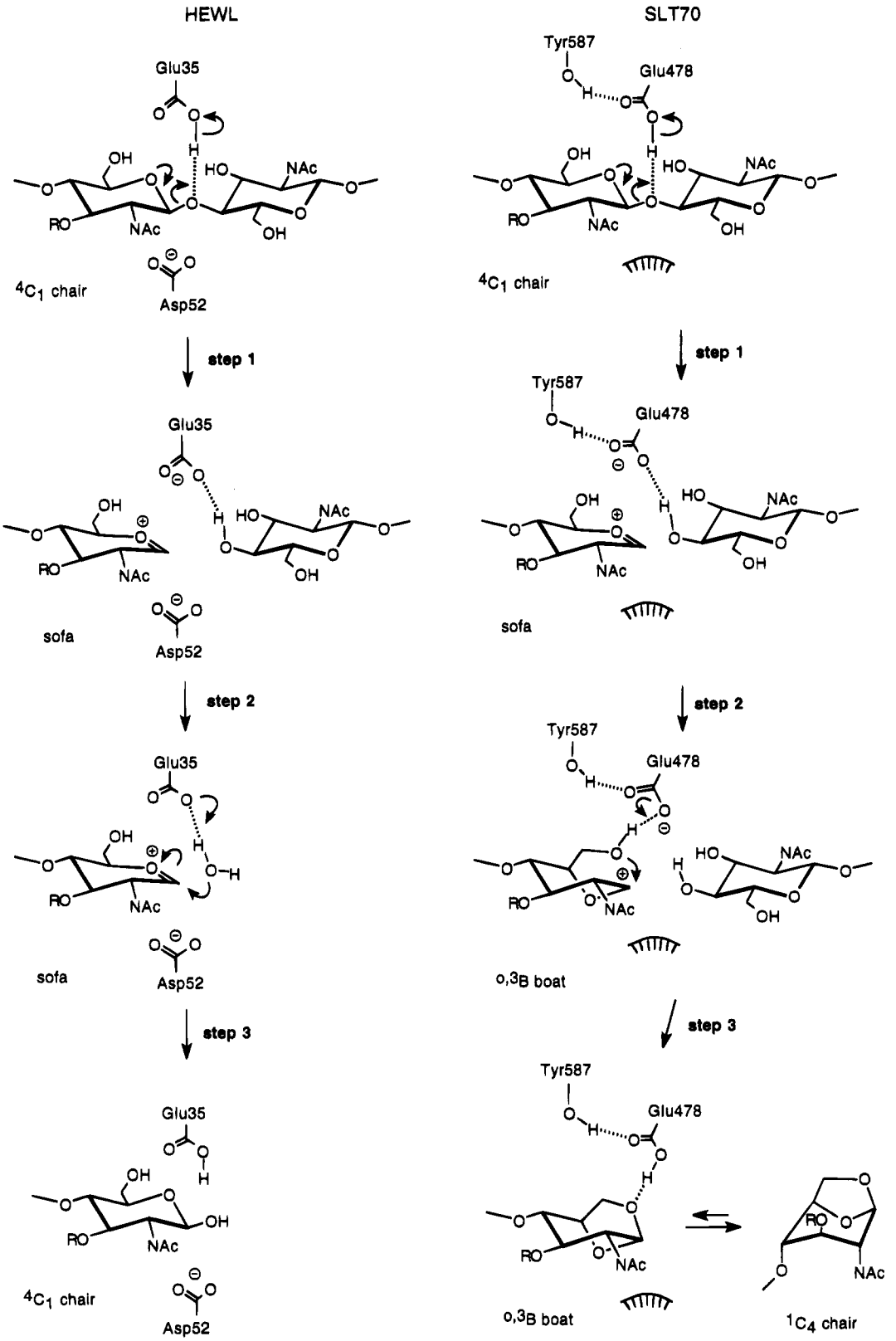

FIGURE 5: Proposed steps in the catalytic mechanism of SLT70 compared to the general-acid catalytic pathway of HEWL, as proposed by Phillips (1967). Glu478 in SLT70 is the equivalent of Glu35 in HEWL. However, there is no equivalent in SLT70 for Asp52 in HEWL (Thunnissen et al., 1994, 1995). The nomenclature of the different conformations of the sugar ring follows the IUPAC rules (Schwarz, 1973).

lent to the Cδ-hydroxymethyl group of bulgecin and is able to make a similar hydrogen bond interaction with Glu478. In fact, in the T4L–muropeptide complex, the 5-hydroxymethyl group of the MurNAc makes such a hydrogen bond with the "catalytic" Glu of T4L (Kuroki et al., 1993). If the MurNAc in subsite D adopts a normal chair conformation, it is impossible to obtain the same spatial overlaps. The only unfavorable contact observed is for the O7 carbonyl atom of the MurNAc 2-acetamido group, which clashes with the side chain of Glu583. However, a rotation about the C2–

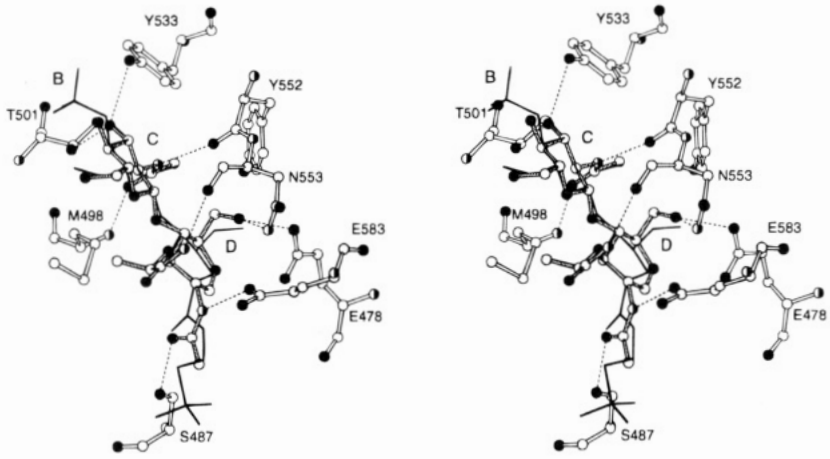

FIGURE 6: Stereodiagram showing a superposition of the GlcNAc−MurNAc cell wall fragment that is covalently linked to the active site of a T4L mutant (Kuroki et al., 1993) and bulgecin as found in the SLT70−bulgecin complex. GlcNAc−MurNAc is shown in ball-and-stick representation, bulgecin in bonds only. The four-residue peptide, which is linked to the lactyl group of MurNAc, has been omitted. The superposition is based on the optimal fit of the GlcNAc residues. No rotations were applied around the glycosidic bond between the GlcNAc and MurNAc residue. Only the 2-acetamido group of the MurNAc was reoriented such that it shows optimal correspondence with the bulgecin atoms. Possible hydrogen bonds between the disaccharide and active site residues of SLT70 are indicated with dotted lines. Atom representations as in Figure 3A.

N2 bond in MurNAc will not only remove this bad contact but may bring the acetamido group in a position allowing it to make interactions similar to those observed in the SLT70−bulgecin complex. With a C1−C2−N7−C7 torsion angle of ~−50°, and the C7−O8 bond cis to N2−C2, the N2 atom of the acetamido group of MurNAc occupies a position close to the N3 atom of bulgecin, and it is within hydrogen-bonding distance to the Oϵ2 of Glu583, while the acetamido O7 atom is spatially close to the carbonyl O atom of bulgecin and may form a hydrogen bond to Ser487. Interestingly, this alternative conformation of the acetamido group allows for an intramolecular participation of this substituent in the SLT70-catalyzed glycosyl transferase reaction. The proposed interaction of the negatively charged Glu583 with the amide of the acetamido group would induce a positive charge on the amide nitrogen and a negative charge on the carbonyl oxygen. Since the carbonyl oxygen is located under the pyranose ring ~3 Å from the C1 atom, the interaction between its negative charge and the (partial) positive charge on the C1 atom may provide extra stabilization of the oxocarbonium ion (Figure 7). Such an intramolecular participation of the 2-acetamido group has been established from studies on the nonenzymatic hydrolysis of glycosides (Piszkiewicz & Bruice, 1968). It has even been suggested as an alternative mechanism for the HEWL-catalyzed reaction (Lowe, 1967), but so far no evidence for such a model has been reported. However, it forms a very interesting hypothesis for the mechanism of the SLT70-catalyzed reaction. It would offer an additional explanation why SLT70 does not need a catalytic aspartate in the active site. The interaction of the acetamido carbonyl O7 and the C1 carbon might also explain why the boat form of the oxocarbonium ion intermediate is favored (Figure 7). Further stabilization of the boat form may be provided through the binding of the peptide that is linked to the MurNAc residue. The interaction between the acetamido group and C1 would also provide sufficient shielding of the oxocarbonium ion from solvent at the C1 atom during the reaction. It may even be argued that the acetamido group captures the oxocarbonium ion to form an oxazoline intermediate, with a covalent bond between C1 and the oxygen of the acetamido group, which is then attacked from the "top" by the C6-hydroxyl group to yield the 1,6-anhydro product. To identify whether the proposed mechanism occurs in SLT70 will require further investigation.

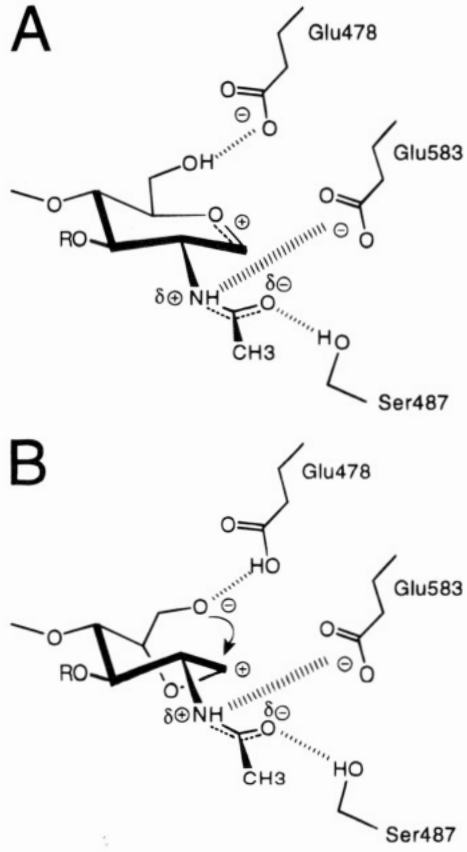

FIGURE 7: Possible structures of MurNAc intermediates in the SLT70-catalyzed cleavage reaction with nucleophilic participation by the oxygen of the 2-acetamido group. In (A) the MurNAc oxocarbonium ion adopts a sofa conformation, in (B) a boat conformation. The interactions with Glu583 and Ser487 promote a conformation for the 2-acetamido group in which the carbonyl oxygen atom may approach the C1 atom of MurNAc. The interaction between the partially negatively charged oxygen atom of the acetamido group and the positive C1 atom may help to stabilize the oxocarbonium ion intermediate and may shield the α-face of C1 from attack by a water molecule.

The 3D structure of the SLT70−bulgecin A complex has not only increased our understanding of the catalytic mechanism of SLT70 but should also permit the rational design of more effective lytic transglycosylase inhibitors. On a speculative note, such inhibitors might enhance the efficacy of already existing β-lactam antibiotics and, therefore, may even prove to be useful against penicillin-resistant bacteria.

ACKNOWLEDGMENT

We thank B. Matthews for the coordinates of the T4L−muropeptide complex prior to deposition in the Brookhaven Data Bank. Takeda Chemical Industries Ltd, Osaka, is thanked for their supply of bulgecin A. We thank K. S. Wilson and staff for providing excellent data collection facilities at the EMBL outstation at DESY, Hamburg.

REFERENCES

Beachey, E. H., Keck, W., de Pedro, M. A., & Schwarz, U. (1981) *Eur. J. Biochem. 116*, 355−358.
Betzner, A. S., & Keck, W. (1989) *Mol. Gen. Genet. 219*, 489−491.
Blake, C. C. F., Johnson, L. N., Mair, G. A., North, A. C. T., Phillips, D. C., & Sarma, V. R. (1967) *Proc. R. Soc. London B 167*, 378−388.
Brünger, A. T. (1992a) *XPLOR 3.0*, Yale University, New Haven, CT 06511.
Brünger, A. T. (1992b) *Nature 355*, 472−474.
Collaborative Computational Project Number 4 (1994) *Acta Crystallogr. D50*, 760−763.
Dijkstra, B. W., & Thunnissen, A.-M. W. H. (1994) *Curr. Opin. Struct. Biol. 4*, 810−813.
Engel, H., Kazemier, B., & Keck, W. (1991) *J. Bacteriol. 173*, 6773−6782.
Engel, H., Smink, A. J., van Wijngaarden, L., & Keck, W. (1992) *J. Bacteriol. 174*, 6394−6403.
Engh, R. A., & Huber, R. (1991) *Acta Crystallogr. A47*, 392−400.
Hadfield, A. T., Harvey, D. J., Archer, D. B., MacKenzie, D. A., Jeenes, D. J., Radford, S. E., Lowe, G., Dobson, C. M., & Johnson, L. N. (1994) *J. Mol. Biol. 243*, 856−872.
Hall, H. K. (1957) *J. Am. Chem. Soc. 79*, 5444−5447.
Handbook of Biochemistry, Selected Data for Molecular Biology (1968) (Sober, H. A., ed.) p J-115, The Chemical Rubber Co., Cleveland, OH.
Hardy, L. W., & Poteete, A. R. (1991) *Biochemistry 30*, 9457−9463.
Hol, W. G. J. (1985) *Prog. Biophys. Mol. Biol. 45*, 149−195.
Höltje, J.-V., & Tuomanen, E. I. (1991) *J. Gen. Microbiol. 137*, 441−454.
Höltje, J.-V., Mirelman, D., Sharon, N., & Schwarz, U. (1975) *J. Bacteriol. 124*, 1067−1076.
Jones, T. A., Zou, J.-Y., Cowan, S. W., & Kjeldgaard, M. (1991) *Acta Crystallogr. A47*, 110−119.
Kabsch, W. (1988) *J. Appl. Crystallogr. 21*, 916−924.
Keck, W., Wientjes, F. B., & Schwarz, U. (1985) *Eur. J. Biochem. 148*, 493−497.
Kitano, K., Tuomanen, E., & Tomasz, A. (1986) *FEMS Microbiol. Lett. 7*, 759−765.
Koshland, D. E. (1953) *Biol. Rev. 28*, 416−420.
Kraulis, P. J. (1991) *J. Appl. Crystallogr. 24*, 946−950.
Kuroki, R., Weaver, L. H., & Matthews, B. W. (1993) *Science 262*, 2030−2033.
Kusser, W., & Schwarz, U. (1980) *Eur. J. Biochem. 103*, 277−281.
Laskowski, R. A., MacArthur, M. W., Moss, D. S., & Thornton, J. M. (1993) *J. Appl. Crystallogr. 26*, 283−291.
Lowe, G. (1967) *Proc. R. Soc. London B 167*, 431−434.
Messerschmidt, A., & Pflugrath, J. W. (1987) *J. Appl. Crystallogr. 20*, 306−315.
Morris, A. L., MacArthur, M. W., Hutchinson, E. G., & Thornton, J. M. (1992) *Proteins: Struct. Funct. Genet. 12*, 345−364.
Phillips, D. C. (1967) *Proc. Natl. Acad. Sci. U.S.A. 57*, 484−495.
Piszkiewicz, D., & Bruice, T. C. (1968) *J. Am. Chem. Soc. 90*, 5844−5848.
Read, R. J. (1986) *Acta Crystallogr. A42*, 140−149.
Romeis, T., Vollmer, W., & Höltje, J.-V. (1993) *FEMS Microbiol. Lett. 111*, 141−146.
Rozeboom, H. J., Dijkstra, B. W., Engel, H., & Keck, W. (1990) *J. Mol. Biol. 212*, 557−559.
Schwarz, J. C. P. (1973) *J. Chem. Soc., Chem. Commun.* 505−508.
Shinagawa, S., Kasahara, F., Wada, Y., Harada, S., & Asai, M. (1984) *Tetrahedron 40*, 3465−3470.
Shinagawa, S., Maki, M., Kintaka, K., Imada, A., & Asai, M. (1985) *J. Antibiot. 38*, 17−23.
Strynadka, N. C. J., & James, M. N. G. (1991) *J. Mol. Biol. 220*, 440−424.
Templin, M. F., Edwards, D. H., & Höltje, J.-V. (1992) *J. Biol. Chem. 267*, 20039−20043.
Thunnissen, A. M. W. H., Dijkstra, A., Rozeboom, H. J., Kalk, K., Engel, H., Keck, W., & Dijkstra, B. W. (1994) *Nature 367*, 750−753.
Thunnissen, A. M. W. H., Isaacs, N. W., & Dijkstra, B. W. (1995) *Proteins: Struct. Funct. Genet. 22*, 245−258.
Ursinus, A., & Höltje, J.-V. (1994) *J. Bacteriol. 176*, 338−343.
Wakamiya, T., Yamanoi, K., Kanou, K., & Shiba, T. (1987) *Tetrahedron Lett. 28*, 5887−5888.
Weaver, L. H., Grütter, M. G., Remington, S. J., Gray, T. M., Isaacs, N. W., & Matthews, B. W. (1985) *J. Mol. Evol. 21*, 97−111.
Weaver, L. H., Grütter, M. G., & Matthews, B. W. (1995) *J. Mol. Biol. 245*, 54−68.